

PAPER • OPEN ACCESS

Observed winds alone cannot explain recent Arctic warming and sea ice loss

To cite this article: Ash L Gilbert *et al* 2025 *Environ. Res.: Climate* **4** 045009

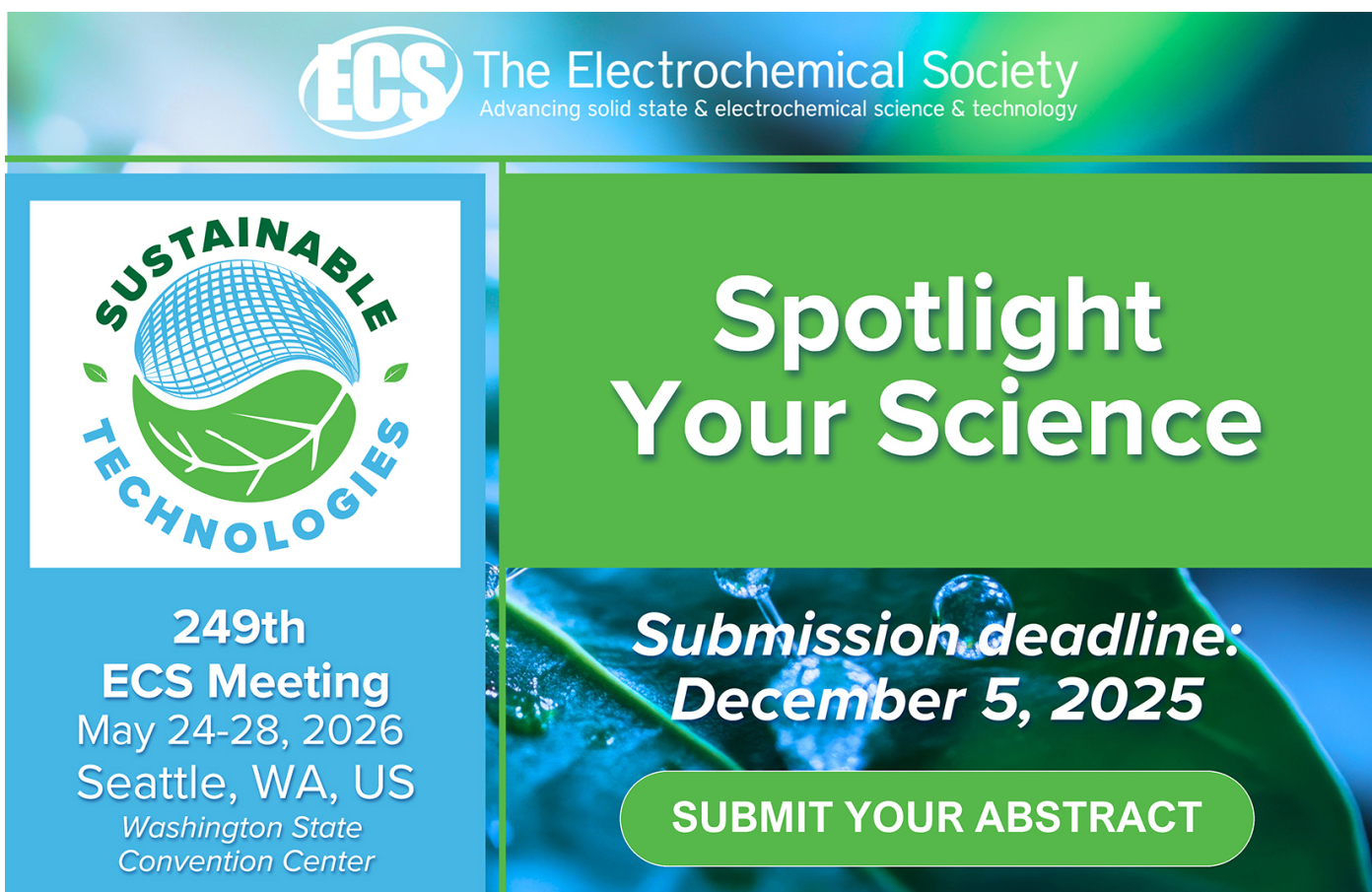
View the [article online](#) for updates and enhancements.

You may also like

- [Electrochemical Advances in Fluorinated/Chlorinated Boron Subphthalocyanines \(BsubPcs\) and Tetrabenzotriazacorroles \(TBCS\) Enabled By the Exploration of Their Base Chemistry and Their Application in Organic Voltaics](#)
Timothy P Bender

- [Effect of Operating Temperature in Li-Air Cells](#)
Jin-Bum Park, Won Jin Kwak, Jusef Hassoun et al.

- [Boron Subphthalocyanines, Boron Subnaphthalocyanines and Silicon Phthalocyanines As Non-Fullerene Electron Accepting Materials in Organic Photovoltaics \(and Tetrabenzo\[corroles as Complimentary Electron Donating Materials\)](#)
Timothy P Bender



The advertisement features the ECS logo and the text "The Electrochemical Society Advancing solid state & electrochemical science & technology". On the left, there's a graphic for "SUSTAINABLE TECHNOLOGIES" featuring a stylized globe and leaves. Below it, details for the "249th ECS Meeting" are provided: "May 24-28, 2026 Seattle, WA, US Washington State Convention Center". On the right, a large green section has the text "Spotlight Your Science" and "Submission deadline: December 5, 2025". A button at the bottom right says "SUBMIT YOUR ABSTRACT".

ENVIRONMENTAL RESEARCH

CLIMATE



PAPER

OPEN ACCESS

RECEIVED

9 May 2025

REVISED

5 September 2025

ACCEPTED FOR PUBLICATION

10 October 2025

PUBLISHED

24 October 2025

Original Content from
this work may be used
under the terms of the
[Creative Commons
Attribution 4.0 licence](#).

Any further distribution
of this work must
maintain attribution to
the author(s) and the title
of the work, journal
citation and DOI.



Observed winds alone cannot explain recent Arctic warming and sea ice loss

Ash L Gilbert^{1,2,*} , Jennifer E Kay^{1,2} , Edward Blanchard-Wrigglesworth³ , David A Bailey⁴ , Marika M Holland⁴ , Alexandra Jahn^{1,5} and David P Schneider²

¹ Department of Atmospheric and Oceanic Sciences, University of Colorado at Boulder, Boulder, CO, United States of America

² Cooperative Institute for Research in Environmental Sciences, Boulder, CO, United States of America

³ Department of Atmospheric and Climate Science, University of Washington, Seattle, WA, United States of America

⁴ Climate and Global Dynamics Laboratory, National Center for Atmospheric Research, Boulder, CO, United States of America

⁵ Institute of Arctic and Alpine Research, University of Colorado Boulder, Boulder, CO, United States of America

* Author to whom any correspondence should be addressed.

E-mail: ash.gilbert@colorado.edu

Keywords: Arctic, sea ice, internal variability, nudging, large-scale circulation

Supplementary material for this article is available [online](#)

Abstract

Since the 1980s, observations show the Arctic surface has warmed four times more than the global mean. Over the Arctic Ocean, this recent large warming is connected to sea ice loss. While earth system models are useful tools for prediction, exact replication of observed Arctic warming and sea ice loss is not expected in freely-evolving models because of internal climate variability. Previous studies have shown that historical hindcasts with model winds nudged to reanalysis can reproduce recent Arctic warming and sea ice loss. However, the influence of observed winds on these recent Arctic changes in absence of anthropogenic forcing has not been assessed. Here, we show that nudging to recent (1980–2023) observed winds alone in a pre-industrial model experiment does not reproduce the magnitude of observed warming and sea ice extent loss. This means that the large-scale winds are not the primary driver of recently observed large Arctic trends. Yet, the winds do partially reproduce the interannual, seasonal, and spatial variability, especially in spring. We also show that in a pre-industrial climate simulation, these results are largely independent of mean state sea ice thickness. In short, the observed winds drive part of the Arctic temperature and sea ice variability but not long-term trends.

1. Introduction

Since reliable satellite records began in 1979, the Arctic surface has warmed nearly four times more than the global surface (Rantanen *et al* 2022) and Arctic sea ice area has decreased in all months, especially during late summer (Simmonds 2015, Meier *et al* 2021). This Arctic warming (Gillett *et al* 2008, Najafi *et al* 2015) and sea ice loss (Min *et al* 2008, Kay *et al* 2011, Stroeve *et al* 2012, Kirchmeier-Young *et al* 2017, Mueller *et al* 2018) is primarily driven by anthropogenic emissions. In earth system models, both warming and sea ice loss are robust features (Manabe and Stouffer 1980, Holland and Bitz 2003, England *et al* 2021) that are predicted to continue throughout this century (Holland and Landrum 2021). Yet there remains considerable uncertainty in projections of Arctic temperature (e.g. Holland and Landrum 2021) and sea ice conditions (e.g. Jahn *et al* 2024). For these projections, two large sources of uncertainty are inter-model structural differences (Massonnet *et al* 2018, Holland and Landrum 2021) and internal variability (i.e. variability arising intrinsically in the coupled climate system that leads to irreducible uncertainty) (e.g. England *et al* 2019, 2025).

In the Arctic, the winds are an important source of internal climate variability in sea ice conditions (e.g. Francis and Hunter 2007, Ogi and Wallace 2007, Wettstein and Deser 2014, Luo *et al* 2017, Siew *et al* 2024) and temperature (e.g. Sweeney *et al* 2023), as assessed through both observations and models.

Several recent studies have evaluated the combined influence of observed winds and historical anthropogenic forcing on recent Arctic climate change by nudging model winds. One study determined the contribution of the observed atmospheric circulation to September Arctic sea ice decline, and found that summertime circulation trends accounted for up to 60% of the decline (Ding *et al* 2017). Another recent study analyzed the influence of winds on the observed Arctic temperature and sea ice in a earth system model simulation with transient anthropogenic forcing and nudged with observed winds (Roach and Blanchard-Wrigglesworth 2022). Their nudged model reproduced the observed interannual variability and trends of Arctic annual temperature and September sea ice extent more accurately than a freely-evolving climate simulation (Roach and Blanchard-Wrigglesworth 2022). Furthermore, Roach and Blanchard-Wrigglesworth (2022) attributed 20%–25% of the September sea ice loss to observed winds. In short, these studies that use historical anthropogenic forcing attribute 20%–60% of the recent sea ice loss to observed winds.

All this said, the exact amount of Arctic warming and sea ice loss driven by the observed winds remains unknown. Specifically, the influence of observed winds on a pre-industrial Arctic climate has not been studied, since all previous work (Ding *et al* 2017, Roach and Blanchard-Wrigglesworth 2022) has used wind nudging in earth system models with anthropogenic forcing. The influence of the winds on the sea ice depends on the mean state, as thicker sea ice is less responsive to the winds and warming (Holland and Stroeve 2011, Kay *et al* 2022). Furthermore, constraining the model to historical winds reduces the noise of internal variability, enabling the signal of mean state sea ice thickness to be easily detectable with a small ensemble size.

Here, we determine the contribution of historical winds alone to observed Arctic temperature and sea ice by nudging model winds to reanalysis winds. In particular, we examine the influence of the winds in the absence of transient anthropogenic forcing on temperature and sea ice Arctic-wide and regional changes at the annual and seasonal timescales. We also evaluate how the contribution of the winds changes with a mean state increase and decrease in pre-industrial Arctic sea ice thickness. We find that the winds alone explain the most internal variability in the spring and drive less than 20% of long-term trends in annual Arctic temperature and September sea ice extent. In other words, winds cannot explain the magnitude of observed warming or sea ice loss. We also find these results had little dependence on mean state sea ice thickness.

2. Methods

2.1. Model description and nudging dataset

We used the Community Earth System Model Version 2.1.5 (CESM2) (Danabasoglu *et al* 2020), a widely-used and well-documented global earth system model, for all our model experiments. CESM2 has fully coupled atmosphere, land, ocean, and sea ice components. Previous work demonstrates that CESM2 models Arctic climate well (e.g. Danabasoglu *et al* 2020, McIlhattan and L'Ecuyer 2025), despite a few biases (Danabasoglu *et al* 2020, DeRepentigny *et al* 2020, Webster *et al* 2021, Kay *et al* 2022). All of our CESM2 simulations have pre-industrial forcing (e.g. constant 1850 forcing) and $\sim 1^\circ$ horizontal grid resolution. CESM2 also has built-in and well-tested nudging capabilities (Roach and Blanchard-Wrigglesworth 2022, Blanchard-Wrigglesworth *et al* 2023, 2024, Topál and Ding 2023). In this work, we nudged the model winds to reanalysis winds following the methodology of Blanchard-Wrigglesworth *et al* (2021) and Roach and Blanchard-Wrigglesworth (2022). This methodology constrains the large-scale Arctic circulation, while allowing the surface atmosphere to freely respond to changing ice and ocean conditions. Specifically, we nudge the zonal (U) & meridional (V) wind components with 6 hourly ERA5 reanalysis files (European Centre for Medium-Range Weather Forecasts 2019, updated monthly) from 1950 to 2023 (total 74 years) for 60° – 90° N and above 850 hPa.

Atmospheric reanalysis models assimilate all available observations to provide a dynamically consistent estimate of the atmospheric state at each time step. Although reanalyses are derived from observations, they use both models and observations. For readability the use of ‘observed winds’ in the rest of this paper refers to the ERA5 reanalysis winds. ERA5 is a state-of-the art reanalysis with reasonable performance for vertical profiles of Arctic winds (Graham *et al* 2019). That said, we recognize that ERA5 has uncertainties (e.g. Pernov *et al* 2024) that are a limitation to this work.

2.2. Datasets for evaluation

To evaluate our new nudged experiments, we established several baselines. First, we selected several observation-based datasets for comparison with our model runs. We use GISS Surface Temperature Analysis version 4 (GISTEMP) for 2m air temperature anomalies (GISTEMP Team 2024, Lenssen *et al*

Table 1. List of coupled modeling science experiments used in this study. All wind nudging model runs use CESM version 2.1.5. All model compset B1850cmip6 on the standard $\sim 1^\circ$ horizontal grid resolution (f09_g17). See supplement table S1 for initialization.

Name	Description	Duration	Reference
PI-control	Freely-evolving pre-industrial control (1850)	2000 years	Danabasoglu <i>et al</i> (2020)
PI-lessmelt	As in PI-control but with lessmelt modifications (Kay <i>et al</i> 2022)	550 years	Kay <i>et al</i> (2022)
PI-moremelt	As in PI-control but with moremelt modifications	400 years	This work
PInudge	Pre-industrial control with nudging to ERA5 winds from $60\text{--}90^\circ \text{N}$ and above 850 hPa	74 years, 3 ensemble members	This work
PInudge-lessmelt	As in PInudge but with lessmelt modifications (Kay <i>et al</i> 2022)	74 years, 3 ensemble members	This work
PInudge-moremelt	As in PInudge but with moremelt modifications	74 years, 3 ensemble members	This work

2024) and ERA5 reanalysis sea ice concentration and 2m air temperature (European Centre for Medium-Range Weather Forecasts 2019, updated monthly, Hersbach *et al* 2020). We kept the ERA5 data at its original resolution ($0.25^\circ \times 0.25^\circ$) except for the spatial pattern correlations in figures 7, 8 and 13, 14, where we re-gridded the ERA5 to the CESM2 horizontal grid resolution ($\sim 1^\circ$). Second, we sampled the CESM2 pre-industrial control run (PI-control, table 1) to generate a baseline for unforced internal climate variability. To do so, we took 51 random slices from the 2000-year long PI-control run to generate a normal distribution. Each slice is 44 years long to match the wind-nudged runs that we analyze (1980–2023).

We want to highlight that the CESM2 PI-control statistics set the background context for interpretation of our new wind-nudging experiments. Using these statistics and applying Wilks (2016) for significance testing, we find that the observed wind trends (1980–2023) are mostly consistent with the unforced pre-industrial climate of CESM2 (figures S1–S5). In other words, the observed wind trends themselves could occur in the absence of anthropogenic forcing.

2.3. Model spin-up

In our initial CESM2 experiments, we encountered model drift caused by wind nudging. Our first wind-nudged experiment (PiC_UVnudge, table S1) had an initial Arctic surface air temperature state 3 K colder than its pre-industrial control initial condition and displayed a large warming trend (figure 1, labeled as 1st cycle). We also noted an initial cooler global temperature and increased sea ice extent. We were unsure whether this result was signal or model drift, since previous atmosphere and ocean studies have shown that model drift can occur when nudging the winds (Roach *et al* 2022, Topál and Ding 2023, Garcia-Oliva *et al* 2024) and may inhibit the reproduction of long-term trends (Greatbatch *et al* 2012). Therefore, we initialized a second wind nudging experiment (PInudge, table 1) from the first experiment after 57 years of simulation, corresponding to year 2006 in the observed wind data. We selected year 2006 because that year was after the global mean temperature in the first experiment stabilized. If the first experiment results were a signal, we expected the second experiment to exhibit similar temperature trends. If the first experiment results were instead drift, we expected the second experiment to have a much smaller temperature trend. As shown in figure 1, the second experiment (labeled 2nd cycle) did have a smaller temperature trend and so we concluded that our model climate had drift associated with the climate state adjusting to wind nudging.

To remove the drift, we implemented a cycling technique used in ocean modeling. Ocean modeling projects cycle their atmospheric forcing 5–6 times to spin up the ocean so it reaches an equilibrium state for the mixed layer (Griffies *et al* 2014, 2016, Tsujino *et al* 2020). So, we removed the model drift in our experiments using a similar technique. For our first and second cycles, we use the same first and second wind-nudging experiments (PiC_UVnudge and PInudge) discussed previously. To assess whether the second cycle still had model drift, we ran a third cycle (PiC_UVnudge_2006_2000, table S1) initialized from year 2000 of the second cycle. As that third cycle was nearly identical to the second cycle (figure 1),

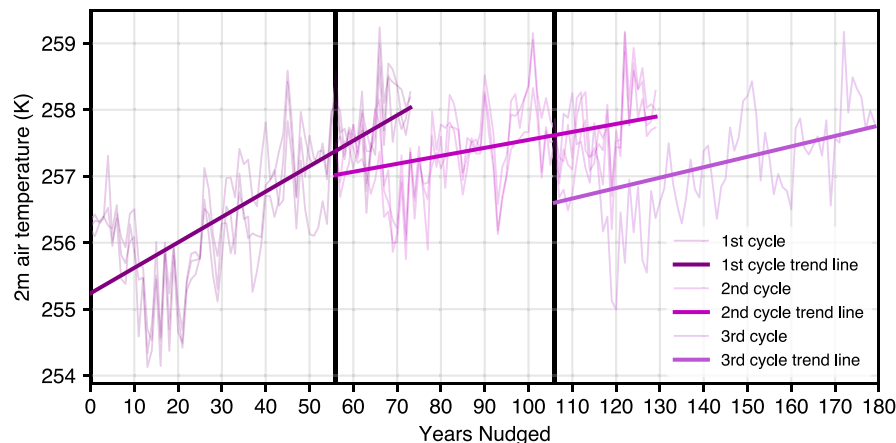


Figure 1. Annual Arctic (70° – 90° N) 2m air temperature for three nudging cycles. Values are plotted as a function of how many years the model climate has been nudged. The first cycle (experiment PiC_UVnudge) ensemble (dark purple) was initialized from the PI-control. The second cycle (experiment PInudge) ensemble (purple) was initialized from year 2006 of the first cycle. The third cycle (experiment PiC_UVnudge_2006_2000) (light purple) was initialized from year 2000 of the second cycle. Vertical black lines indicate when a new model run was initialized. All model experiments have the trend line for the ensemble mean plotted. See table 1 for model experiment details.

we concluded that the model drift had been removed in the second cycle and we proceeded to use that cycle in the following experiments.

2.4. Model science experiments

A complete list of the CESM2 experiments used in this study is available in table 1. All nudging experiments are ensembles in order to sample the internal variability of the wind-nudged pre-industrial climate system. Our first new science experiment run (PInudge) addresses the influence of the observed winds alone on the Arctic climate state in absence of anthropogenic forcing. PInudge has three ensemble members that each span 74 years (length of observed wind timeseries) with model winds nudged according to our nudging procedure (table 1). Our second (PInudge-lessmelt) and third (PInudge-moremelt) science experiments address the contribution of the winds plus a mean state change in sea ice thickness. Both experiments have the same experimental set-up as PInudge: pre-industrial forcing nudged with observed winds. The only difference lies in the sea ice model component, such that PInudge-lessmelt has thicker sea ice and PInudge-moremelt has thinner sea ice (table 1).

The mean state sea ice thickness changes in PInudge-lessmelt and PInudge-moremelt were generated by parameter modifications. For PInudge-lessmelt, we followed Kay *et al* (2022), whom modified parameters within the CESM2 sea ice model component to produce thicker (figures S7(b) and (e)) and more expansive sea ice (figures S8(b) and (e)) and a colder climate. For PInudge-moremelt, there were no previously developed CESM2 parameter combinations for thinner sea ice in a pre-industrial control. So, we created our own set of ‘moremelt’ parameter modifications by tuning a pre-industrial control (PI-moremelt) to have thinner sea ice. Initialized from the PI-control at year 811, PI-moremelt is a 400 year long control run identical to the existing PI-control (Danabasoglu *et al* 2020) except for a single parameter change. In the sea ice component of CESM2 (CICE), we decreased the r_{snw} parameter from 1.25 to 0.0 standard deviations, thus increasing the dry snow grain radius from $187.5 \mu\text{m}$ to $500 \mu\text{m}$. This large snow grain radius increase in PI-moremelt decreased the dry snow albedo and in doing so, it decreased the mean sea ice thickness (figures S7(c) and (f)), sea ice extent (figure 2(a); figures S8(c) and (f)), and sea ice volume (figure 2(b)).

3. Results

3.1. Influence of observed winds on modeled Arctic surface temperature and sea ice

We first examine the influence of the observed Arctic winds alone on annual mean Arctic temperature using the wind-nudging experiment PInudge (table 1). The three PInudge ensemble members cannot reproduce the magnitude of the observed annual Arctic warming between 1980 and 2023 (figure 3). The PInudge ensemble simulates an annual temperature trend of 0.11 K dec^{-1} , much smaller than the observed trend of 0.71 K dec^{-1} (figure 4). However, the PInudge ensemble members explain 21% of the observed interannual temperature variability (figure 3). Finally, these ensemble members are mostly

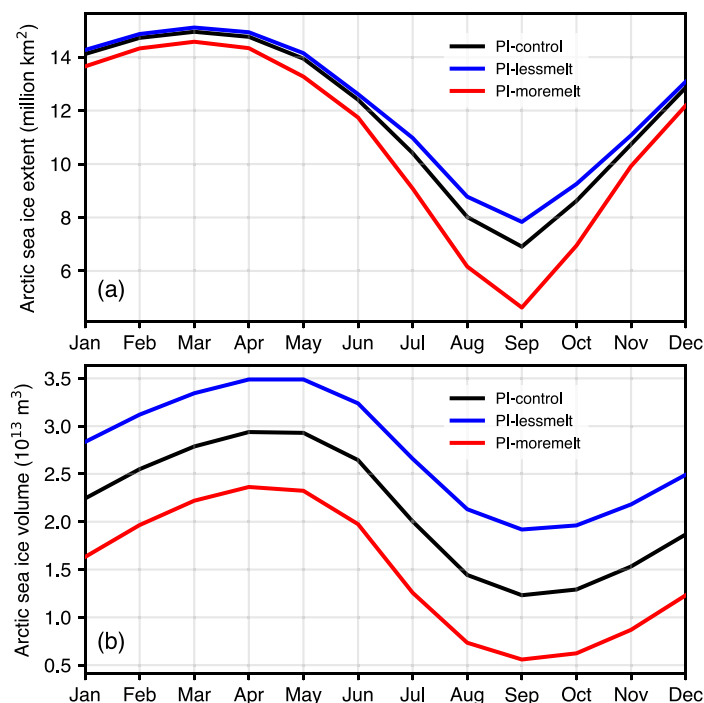


Figure 2. Seasonal cycles of the PI-control, PI-lessmelt, and PI-moremelt for (a) Arctic sea ice extent and (b) Arctic sea ice volume. The seasonal cycles are averaged over years 911–1110.

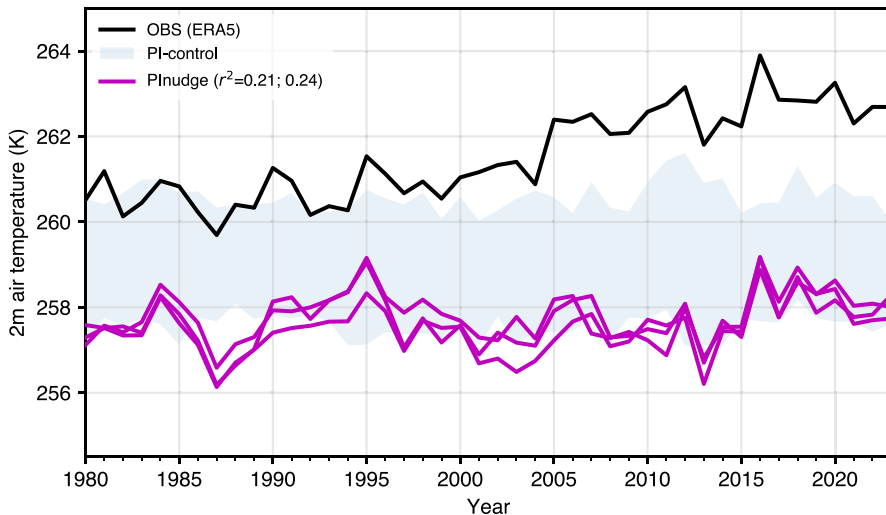


Figure 3. Annual Arctic (70°–90° N) 2m air temperature timeseries (1980–2023) for observations (ERA5 reanalysis), PI-control, and PI-nudge. The bounds of PI-control are the absolute maxima and minima of the sample for each year. Wind-nudged experiment (PI-nudge) is plotted as a function of the nudged wind year. Coefficients of determination (annual temperature; detrended anomalies) are between wind-nudged experiment ensemble mean and ERA5.

within the spread of the pre-industrial control (PI-control). Thus, the observed winds had little influence on the mean state temperature.

The Arctic has strong seasonality, so we next assess observed and modeled temperature trends by month (figure 4(a)). We find that PI-nudge temperature trends (44 years with 1980–2023 winds) are smaller than the observed trends in every month. This result suggests that the observed winds contribute little to observed temperature trends regardless of the month. Furthermore, both annual and monthly temperature trends for PI-nudge are within the pre-industrial range. Yet despite simulating weak temperature trends, PI-nudge has more warming in the late fall through spring, in agreement with observations. In spring, PI-nudge explains the most warming, about 40% of the observed trend for the months of April

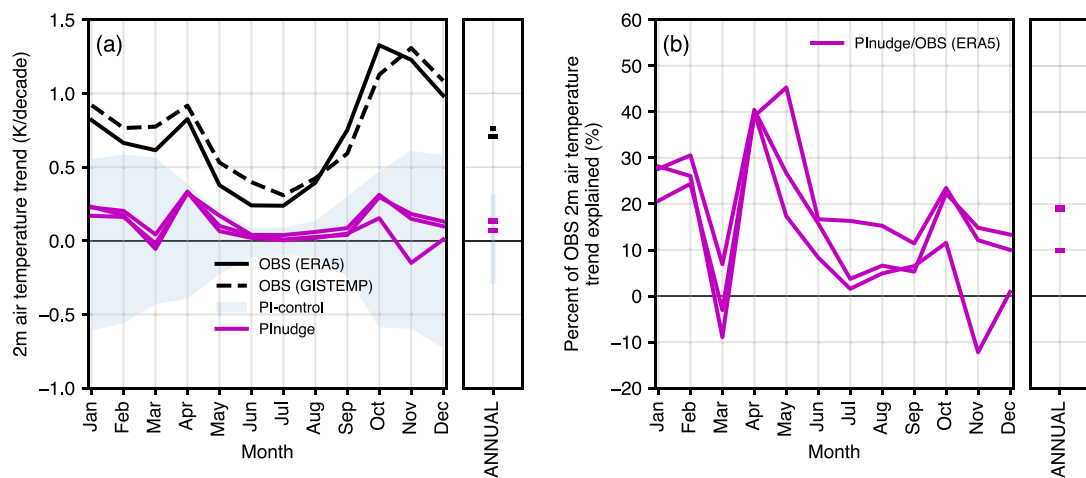


Figure 4. (a) Monthly and annual trends (1980–2023) in Arctic (70° – 90° N) 2m air temperature for observations (ERA5 reanalysis and GISTEMP), PI-control, and PInudge. The bounds of PI-control are the absolute maxima and minima of the sample trends. (b) Percent of observed (ERA5 reanalysis) monthly and annual Arctic 2m air temperature trends explained by PInudge.

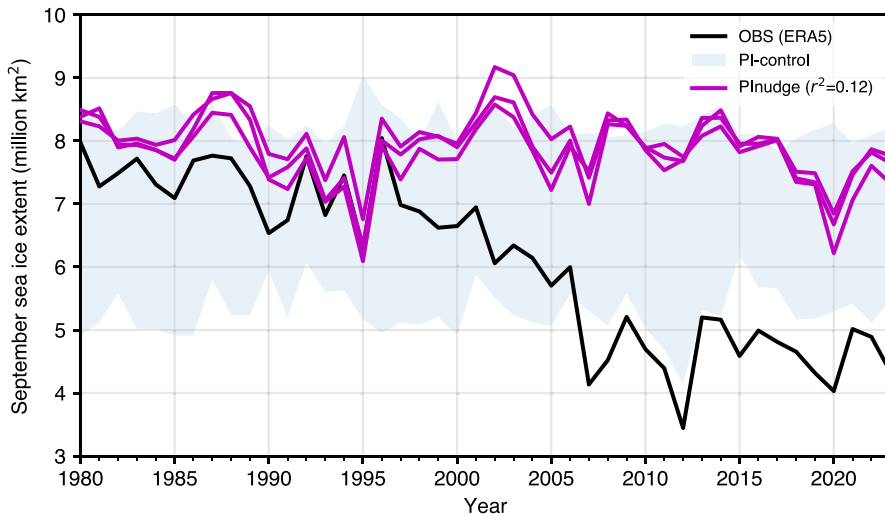


Figure 5. September Arctic sea ice extent timeseries (1980–2023) for observations (ERA5 reanalysis), PI-control, and PInudge. The bounds of PI-control are the absolute maxima and minima of the sample for each year. Coefficients of determination are between wind-nudged experiment ensemble mean and ERA5.

and May (figure 4(b)). In summer, PInudge temperature trends are near-zero. In short, the observed winds have some influence on the seasonal pattern of warming, with the strongest influence in spring months.

Next, we evaluate the contribution of the winds to the seasonal sea ice minimum in September (figure 5). The PInudge ensemble does not reproduce the observed (1980–2023) September Arctic sea ice loss. Specifically, PInudge simulates a September sea ice extent loss of $0.10 \text{ million km}^2 \text{ dec}^{-1}$, in contrast to the observed loss of $0.92 \text{ million km}^2 \text{ dec}^{-1}$ (figure 6). Though, PInudge captures 12% of the September sea ice interannual variability. Additionally, PInudge sea ice extent is mostly within the pre-industrial control climate. So like the annual Arctic temperature, the observed winds have little influence on the mean state September sea ice extent.

Having assessed sea ice at the seasonal minimum, we expand to consider the Arctic sea ice extent trends in all months and annually (figure 6(a)). All monthly sea ice extent trends in PInudge are much smaller in magnitude than observed trends. Indeed, all PInudge sea ice trends are less than $0.10 \text{ million km}^2 \text{ dec}^{-1}$, whereas the smallest observed sea ice loss in any month is $0.36 \text{ million km}^2 \text{ dec}^{-1}$. Furthermore, monthly PInudge sea ice trends are consistent with the pre-industrial control. These results indicate that the observed winds have little influence on monthly sea

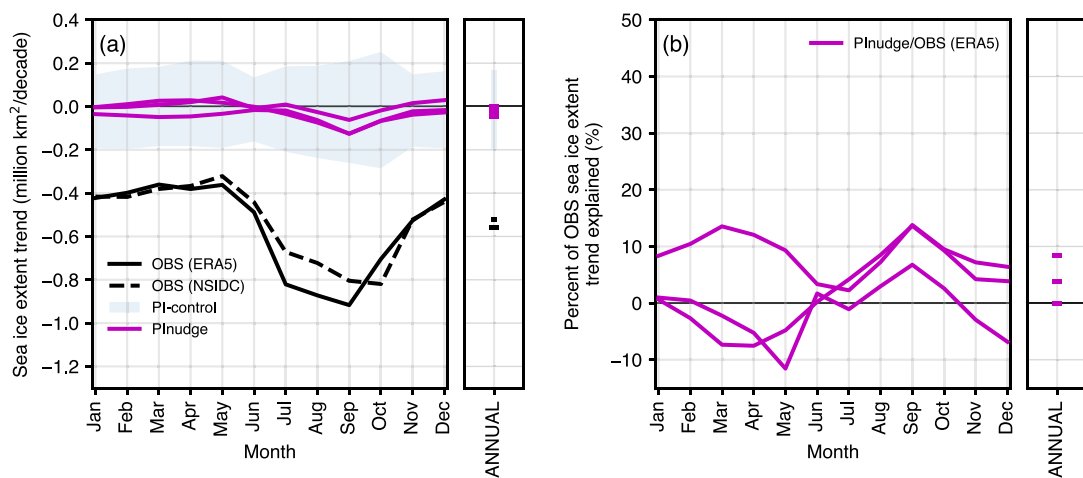


Figure 6. (a) Monthly and annual trends (1980–2023) in Arctic sea ice extent for observations (ERA5 reanalysis), PI-control, and PInudge. The bounds of PI-control are the absolute maxima and minima of the sample trends. (b) Percent of observed (ERA5 reanalysis) monthly and annual Arctic sea ice extent trends explained by PInudge.

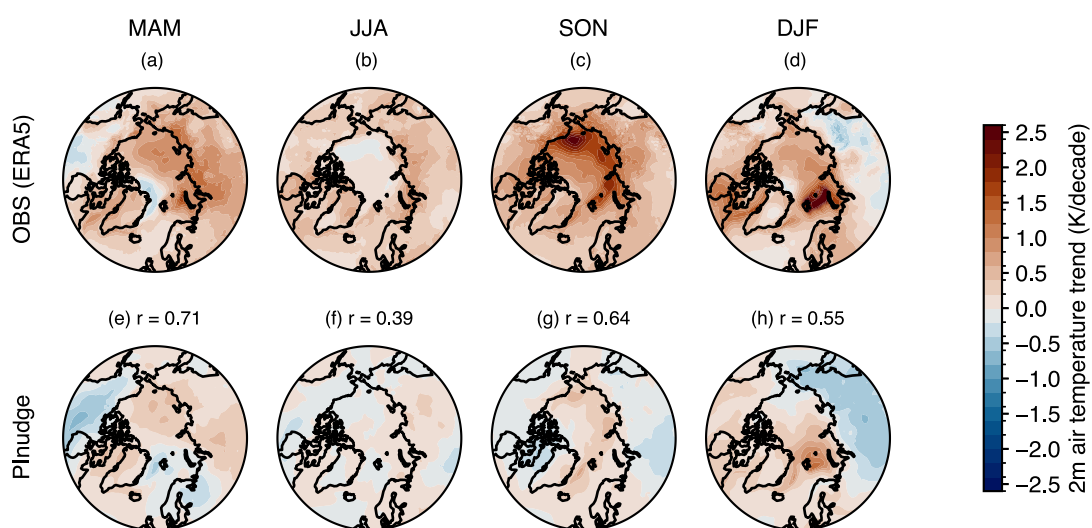


Figure 7. Local 2m air temperature trends (1980–2023): (a) Observed (ERA5) MAM, (b) Observed JJA, (c) Observed SON, (d) Observed DJF, (e)–(h) as in (a)–(d) but for the PInudge ensemble mean. Pattern correlations between observations and PInudge are provided. Stippling on (e)–(h) indicates PInudge differs from PI-control sample at the 95% confidence level. False discovery rate was controlled for using Wilks (2016). The colormaps are generated based on work by Crameri *et al* (2020).

ice loss (figure 6(b)). However, PInudge has more sea ice loss in late summer compared to the rest of the year.

Since changes in the Arctic are highly location dependent, we next describe local surface temperature trends for each season in PInudge (figure 7). In every season, the observed warming (figures 7(a)–(d)) is larger than the PInudge ensemble mean (figures 7(e)–(h)). For example, the largest observed warming in SON is 2.6 K dec^{-1} , whereas the warming in the same region of PInudge is only 0.6 K dec^{-1} (figures 7(c) and (g)). Moreover, none of the local PInudge temperature trends are significantly different than the PI-control, in any season. Thus, based on these comparisons, the observed winds cannot explain the strength of local temperature trends.

While the magnitude of the warming differs, the regions of strongest warming in PInudge and the observations are often in agreement (figure 7). This similarity in the spatial pattern of warming between the observations and PInudge is found in all seasons except summer (JJA). The spatial pattern correlations during MAM (0.71), SON (0.64), and DJF (0.55) are all high. Notably, PInudge reproduces the observed pattern the best in MAM (figures 7(a) and (e)). This result agrees with our earlier finding that PInudge explains the most (40%) observed warming in April and May. Additionally, both PInudge and

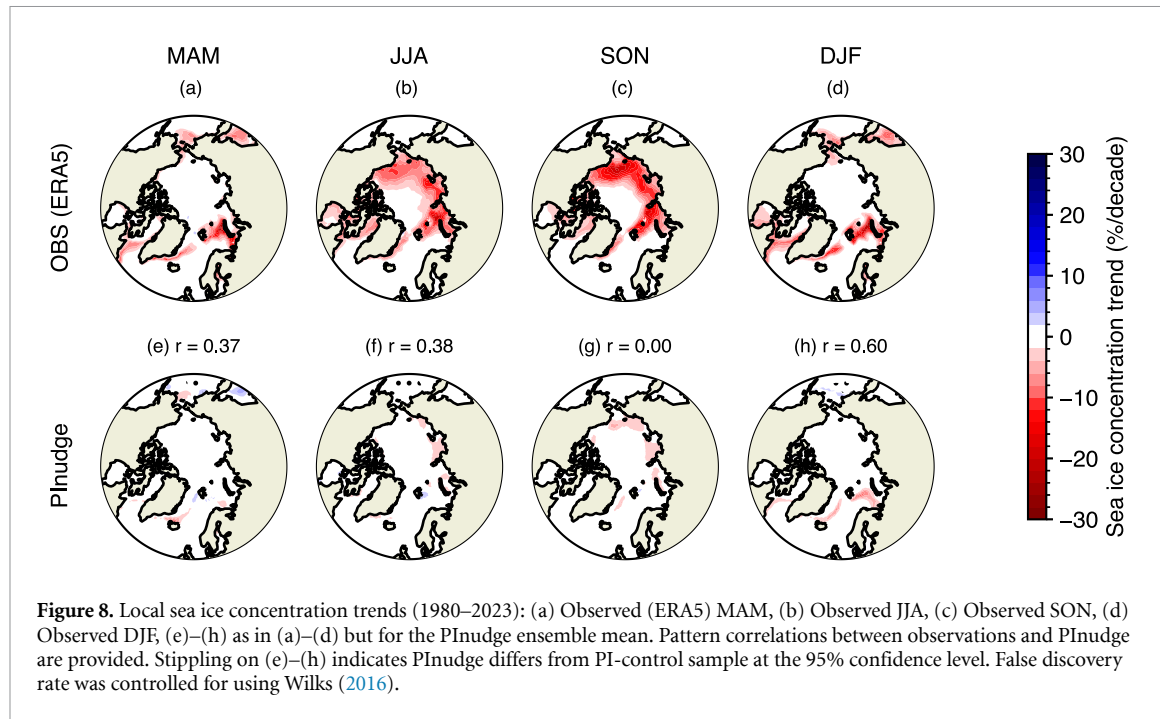


Figure 8. Local sea ice concentration trends (1980–2023): (a) Observed (ERA5) MAM, (b) Observed JJA, (c) Observed SON, (d) Observed DJF, (e)–(h) as in (a)–(d) but for the PInudge ensemble mean. Pattern correlations between observations and PInudge are provided. Stippling on (e)–(h) indicates PInudge differs from PI-control sample at the 95% confidence level. False discovery rate was controlled for using Wilks (2016).

observations have a warm Arctic cold Eurasia (WACE) pattern in DJF (figures 7(d) and (h)). However, PInudge has weaker warming over the Barents and Bering Seas and stronger and more widespread cooling over Russia during DJF. Regardless, this result suggests that the observed WACE pattern is internally driven rather than externally forced (Xu *et al* 2019, He *et al* 2020, Labe *et al* 2020). Furthermore, the observed WACE pattern has been linked to blocking anti-cyclones at the 500 hPa level over northern Europe (Overland *et al* 2015, Luo *et al* 2016). The DJF geopotential heights also show an increase in blocking anti-cyclones northern Europe in both the observations and PInudge, supporting this link (figures S6(a)–(h)). During JJA, the pattern correlation is much lower than during the rest of the year, decreasing to 0.39. The JJA pattern in PInudge differs from observations by showing weak cooling instead of warming over the North Atlantic, North Pacific, and North America (figures 7(b) and (f)). These weak JJA air temperature trends may result from a net heat transfer into the ocean and sea ice (e.g. Serreze *et al* 2009, Screen and Simmonds 2010).

Having compared spatial patterns of temperature trends, we next compare the magnitude of spatial sea ice concentration trends in PInudge and observations (figure 8). In all seasons, the PInudge ensemble mean (figures 8(e)–(h)) fails to reproduce the magnitude of the observed (figures 8(a)–(d)) sea ice loss. For example in the fall (SON), the largest PInudge sea ice loss is 5.1 % dec⁻¹ in the Chukchi Sea, but there the observed sea ice loss is in excess of 20 % dec⁻¹ (figures 8(c) and (g)). Yet besides a few weak sea ice trends (within ± 2 % dec⁻¹) in the Bering Sea, the PInudge trends are not significantly different than the PI-control. Like figure 7, these spatial patterns reinforce that the observed winds cannot explain the sea ice loss magnitude.

Having compared sea ice trend magnitudes, we next analyze sea ice trend spatial patterns (figure 8) and their association with temperature trend spatial patterns (figure 7). The spatial pattern of maximum sea ice loss in PInudge agrees with observations during SON and DJF, but not in MAM and JJA. Similarly, the spatial patterns of sea ice loss and warming match for both the observations and PInudge during SON and DJF but not in MAM and JJA. Based on this analysis, we find that observed winds have some influence on regional patterns of sea ice loss.

3.2. Dependence on mean state sea ice

Next, we assess the influence of thicker (PInudge-lessmelt) and thinner (PInudge-moremelt) mean state sea ice (table 1) on our results. Surprisingly, we find that the sea ice mean state has little impact on our results beyond changing the mean state climate. Similar to PInudge, neither PInudge-lessmelt nor PInudge-moremelt reproduce the magnitude of the observed annual Arctic temperature trend (figure 9). Specifically, PInudge-lessmelt simulates an annual temperature trend of 0.12 K dec⁻¹ and PInudge-moremelt simulates 0.14 K dec⁻¹ (figure 10). Similarly, both PInudge-lessmelt and PInudge-moremelt explain roughly the same amount of interannual variability as PInudge, 19% and 23%, respectively. As

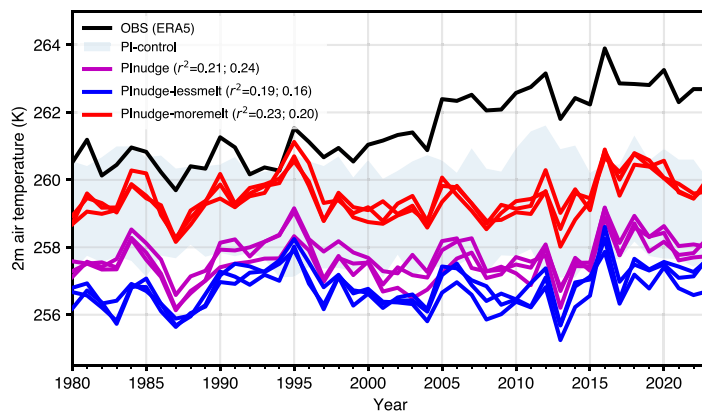


Figure 9. As in figure 3 but also including PI-nudge-lessmelt and PI-nudge-moremelt.

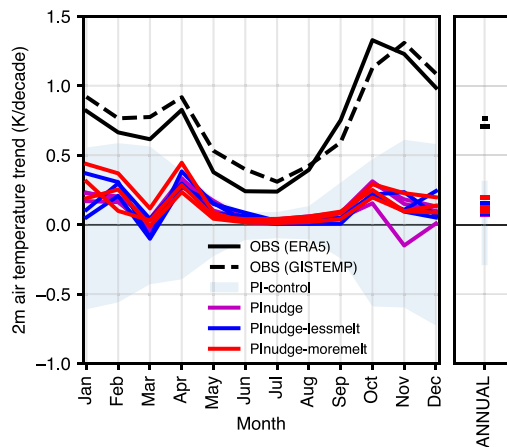


Figure 10. As in figure 4(a) but also including PI-nudge-lessmelt and PI-nudge-moremelt.

for the effect on the mean state Arctic temperature, PI-nudge-lessmelt is 0.9 K cooler than PI-nudge and 2.2 K cooler than the pre-industrial climate, whereas PI-nudge-moremelt is 1.8 K warmer than PI-nudge and 0.45 K warmer than the pre-industrial climate. These mean state changes result in PI-nudge-lessmelt being cold enough to be inconsistent with the PI-control, but PI-nudge-moremelt is still mostly within the PI-control spread.

Like temperature, PI-nudge-lessmelt and PI-nudge-moremelt have different September mean state sea ice extents (figure 11). PI-nudge-lessmelt has more September sea ice than PI-nudge, whereas PI-nudge-moremelt has less September sea ice than PI-nudge. But, the magnitude of the modeled sea ice trends and interannual variability are similar in PI-nudge, PI-nudge-lessmelt, and PI-nudge-moremelt. Thus, sea ice mean state has little impact on the influence of observed winds on the simulated September sea ice trends.

Re-enforcing that the mean state of the sea ice has little influence on our results, we finally compare the trends by month and spatially. For both monthly temperature (figure 10) and sea ice extent (figure 12) trends, PI-nudge, PI-nudge-lessmelt, and PI-nudge-moremelt are nearly indistinguishable. While small, it is worth noting that PI-nudge-moremelt simulates 50% larger sea ice loss than both PI-nudge and PI-nudge-lessmelt (figure 12). PI-nudge-moremelt still explains only 16% of the observed trend (figure S10). In every season, both PI-nudge-lessmelt (figures 13(a)–(d); figures 14(a)–(d)) and PI-nudge-moremelt (figures 13(e)–(h); figures 14(e)–(h)) resemble the spatial temperature and sea ice trend patterns from PI-nudge (figures 7(e)–(h); figures 8(e)–(h)).

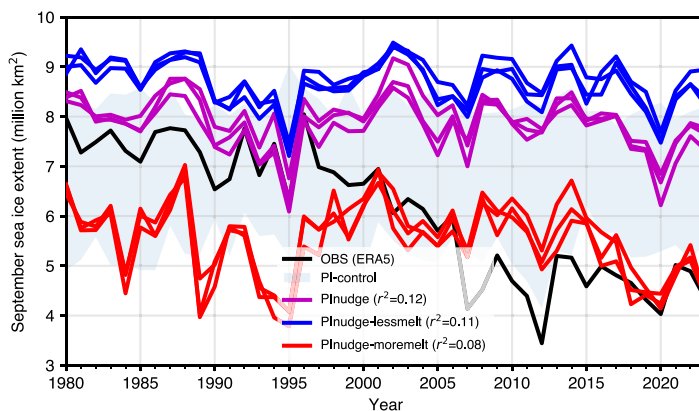


Figure 11. As in figure 5 but also including PI-nudge-lessmelt and PI-nudge-moremelt.

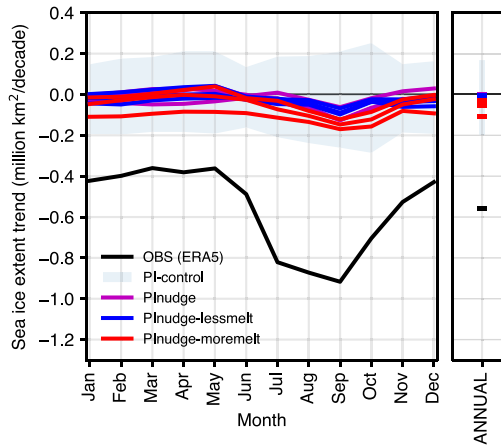


Figure 12. As in figure 6(a) but also including PI-nudge-lessmelt and PI-nudge-moremelt.

4. Discussion

Our study found that in absence of anthropogenic forcing, observed winds cannot explain recent (1980–2023) Arctic warming or sea ice loss on monthly or annual time scales and on pan-Arctic or regional spatial scales. The observed warming and sea ice loss explained the wind-nudged experiments is smaller, at most 16%, in contrast to other studies that attribute 20% to 60% (Ding *et al* 2017, Roach and Blanchard-Wrigglesworth 2022). Additionally, all of the PI-nudge, PI-nudge-lessmelt, and PI-nudge-moremelt trends are consistent with the pre-industrial control. In other words, all temperature and sea ice extent trends forced by the winds alone in the wind-nudged experiments could have occurred in a pre-industrial climate without wind nudging. For these reasons, although we do quantify the contribution of the winds to recent Arctic warming and sea ice loss, we do not consider these contributions to be significant. Therefore, this work agrees that atmospheric circulation is not the sole driver of observed warming and sea ice loss (Ding *et al* 2017, Roach and Blanchard-Wrigglesworth 2022).

Another important result is that the winds partially influence observed Arctic temperature and sea ice variability and spatial patterns. For the annual temperature and seasonal sea ice extent minima, the observed winds explain between one-tenth and one-fifth of the interannual variability. The observed winds also drive seasonal patterns of warming and sea ice loss. Our results agree that the observed winds have considerable influence over spring temperature trends (Räisänen 2021). In contrast to prior research, our results suggest the observed winds have little influence on summer temperature and sea ice extent trends (Baxter and Ding 2022). These findings are consistent with other studies evaluating the contribution of winds to observed Arctic warming and sea ice loss (Ding *et al* 2017, Roach and

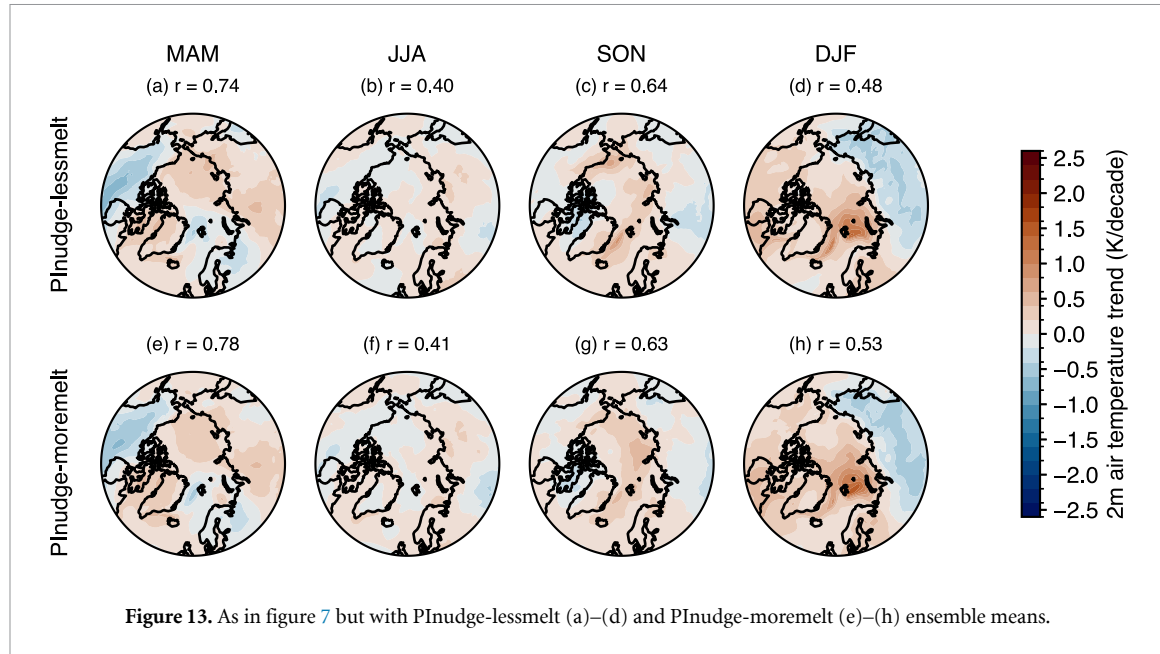


Figure 13. As in figure 7 but with PI nudged-lessmelt (a)–(d) and PI nudged-moremelt (e)–(h) ensemble means.

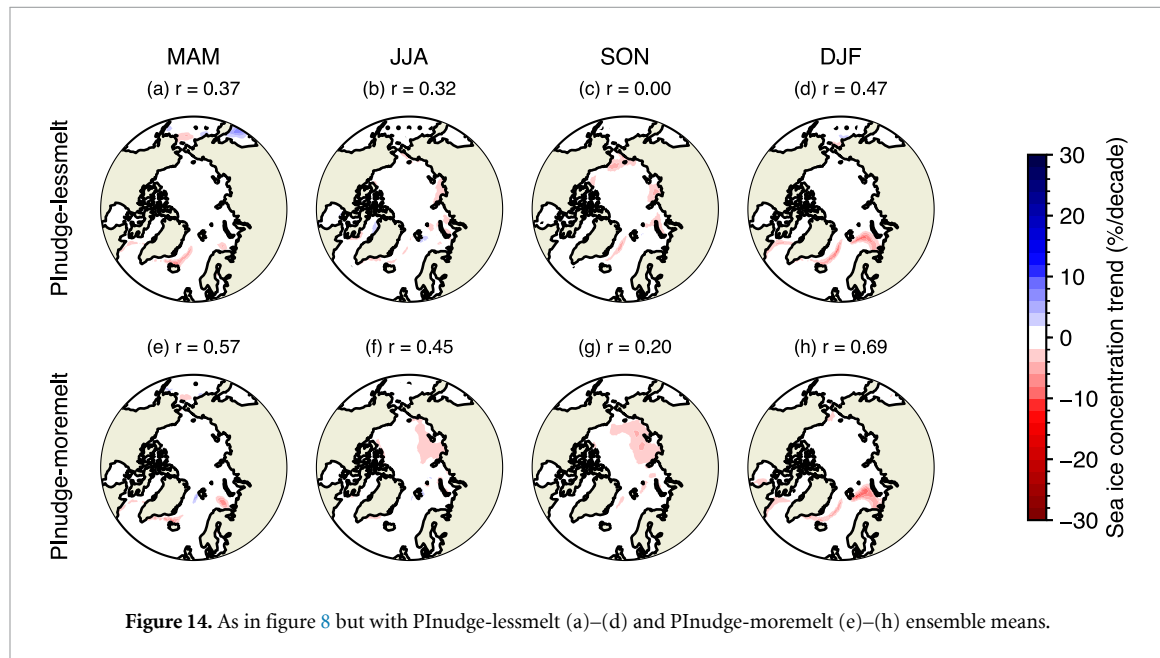


Figure 14. As in figure 8 but with PI nudged-lessmelt (a)–(d) and PI nudged-moremelt (e)–(h) ensemble means.

Blanchard-Wrigglesworth 2022). Furthermore, our results agree that the winds have less influence on sea ice than temperature (Roach and Blanchard-Wrigglesworth 2022).

While the sea ice thickness changes affected mean state temperature and sea ice extent in PI nudged-lessmelt and PI nudged-moremelt, there was limited impact on temperature and sea ice extent trends. The simulated influence of historical Arctic winds on surface air temperature and sea ice variations had no dependence on mean state sea ice thickness. However, PI nudged-moremelt had slightly larger sea ice loss trends in late summer than PI nudged, but not to the extent that the trends were outside the pre-industrial control. Temperature and sea ice regional trend patterns, interannual variability, and seasonal patterns were also unaffected by both the sea ice thickness increase and decrease. We had expected that the thinner sea ice in PI nudged-moremelt would allow the winds to move the sea ice more, causing more melt and warming (e.g. Holland and Stroeve 2011, Kay *et al* 2022). Yet our results refuted this expectation. One possible explanation is that without other changes in the mean state atmosphere ocean, any response from mean state sea ice thickness changes may be dampened. For example, the nudged model winds transport air from lower latitudes. That air is at pre-industrial temperatures, not warmer, historical temperatures. Therefore, atmospheric transport in our simulations may not induce as much sea ice

loss or warming as atmospheric transport in a historical climate. This example can also be applied to the ocean (Zhang *et al* 2013).

There are several limitations to this work. First, we limit our conclusions to the model used in this study, CESM2. Although we recommend replicating this study with other earth system models, we suspect a different earth system model would confirm our conclusions. We base this on the fact that earth system models often differ in mean state, but we tested a mean state change and found no effect on our results. Second, sea ice is thicker in a pre-industrial climate than a historical climate (Kay *et al* 2022). Since thicker sea ice is less responsive to winds (Holland and Stroeve 2011) and wind nudging, our wind-nudged experiments may underestimate the influence of observed winds on sea ice trends. However, we thinned the sea ice to observed historical values in PInudge-moremelt and found no effect on the observed wind contribution. Third, we note the observed winds experienced anthropogenic forcing and indirectly added the forcing to our experiments via wind nudging. From this perspective, our study is not evaluating the influence of the winds alone. However our analysis of observed wind trends in section 2.2 showed that anthropogenic forcing had a negligible effect on the winds. Therefore, we disregard the indirect anthropogenic forcing added during nudging. Finally, we note that the Arctic climate is sparsely observed. While reanalysis winds are constrained by observations, the exact evolution of the historical winds will never be known. However, it is unlikely that the reanalysis has completely missed major variations in historical winds that would drive strong warming or sea ice loss trends.

Future work will be aimed at precisely attributing the roles of anthropogenic forcing and winds on Arctic warming and sea ice loss, using this nudging framework. Indeed, this study provides a novel framework for wind-nudging CESM2 under different boundary conditions, or combinations of external forcings. We have presented a base case that provides clarity on the role of the winds alone. This work will help to constrain projections of Arctic climate by controlling for internal variability when parameterization changes to sea ice thickness (or other aspects of the mean state) are made.

5. Conclusion

In this study, we determined the influence of observed Arctic winds on recent Arctic warming and sea ice loss from pre-industrial climate model experiments nudged with observed winds. We find that, in absence of historical external forcing, the observed winds cannot reproduce the magnitude of recent Arctic warming and sea loss—at most, winds explain 16% of the observed trends. However, the observed winds can partially reproduce Arctic temperature and sea ice interannual, seasonal, and spatial variability. Therefore, we conclude that the atmospheric circulation is not the dominant driver of recent Arctic warming and sea loss but still plays an important role in Arctic climate variability. Finally, we find that our results are largely not dependent on mean state sea ice thickness.

Data availability statement

The full climate model data used in this study are available on National Center for Atmospheric Research Glade Globus Collection at /glade/campaign/univ/ucub0155/glydia. All code to run the model simulations and process and plot the output is available at <https://doi.org/10.5281/zenodo.16884086> (Gilbert 2025a). Data plotted in this paper and its supplement are available at <https://doi.org/10.5281/zenodo.16878063> (Gilbert 2025b).

Acknowledgments

ALG was funded by the National Science Foundation (NSF) Graduate Research Fellowship (Grant No. 2040434) and NSF Office of Polar Programs (OPP) (Grant No. 2233420). JEK was funded by NSF OPP (Grant No. 2233420). EBW was funded by NSF OPP (Grant Nos. 2233421 and 2213988). DAB was supported by the NSF National Center for Atmospheric Research (NCAR), which is a major facility sponsored by the U.S. NSF under Cooperative Agreement No. 1852977. MMH was funded by NSF OPP (Grant No. 2138788). AJ was funded by an NSF CAREER Award (Grant No. 1847398). DPS was funded by NSF OPP (Grant No. 2233420). The authors gratefully acknowledge supercomputing support from the Derecho and Casper systems <https://doi.org/10.5065/qx9a-pg09> provided by the NSF NCAR, sponsored by the NSF (Computational and Information Systems Laboratory (CISL) 2023). All authors thank the NCAR Polar Climate Working Group for helpful feedback.

Conflict of interest

The authors have no conflicts of interest to report.

ORCID iDs

- Ash L Gilbert  0000-0002-8415-364X
Jennifer E Kay  0000-0002-3625-5377
Edward Blanchard-Wrigglesworth  0000-0002-2608-0868
David A Bailey  0000-0002-6584-0663
Marika M Holland  0000-0001-5621-8939
Alexandra Jahn  0000-0002-6580-2579
David P Schneider  0000-0001-5308-1834

References

- Baxter I and Ding Q 2022 An optimal atmospheric circulation mode in the Arctic favoring strong summertime sea ice melting and ice-albedo feedback *J. Clim.* **35** 6627–45
- Blanchard-Wrigglesworth E, Brenner S, Webster M, Horvat C, Ø F and Bitz C M 2024 Model biases in simulating extreme sea ice loss associated with the record January 2022 Arctic cyclone *J. Geophys. Res. Oceans* **129** e2024JC021127
- Blanchard-Wrigglesworth E, Cox T, Espinosa Z I and Donohoe A 2023 The largest ever recorded heatwave—characteristics and attribution of the Antarctic heatwave of March 2022 *Geophys. Res. Lett.* **50** e2023GL104910
- Blanchard-Wrigglesworth E, Roach L A, Donohoe A and Ding Q 2021 Impact of winds and Southern Ocean SSTs on Antarctic sea ice trends and variability *J. Clim.* **34** 949–65
- Computational and Information Systems Laboratory (CISL) 2023 Derecho: HPE Cray EX System (University Community Computing) NSF National Center for Atmospheric Research (NCAR) Boulder, CO (<https://doi.org/10.5065/qx9a-pg09>)
- Cameri F, Shephard G E and Heron P J 2020 The misuse of colour in science communication *Nat. Commun.* **11** 5444
- Danabasoglu G et al 2020 The Community Earth System Model Version 2 (CESM2) *J. Adv. Model. Earth Syst.* **12** e2019MS001916
- DeRepentigny P, Jahn A, Holland M M and Smith A 2020 Arctic sea ice in two configurations of the CESM2 during the 20th and 21st centuries *J. Geophys. Res. Oceans* **125** e2020JC016133
- Ding Q et al 2017 Influence of high-latitude atmospheric circulation changes on summertime Arctic sea ice *Nat. Clim. Change* **7** 289–95
- England M R, Eisenman I, Lutsko N J and Wagner T J W 2021 The recent emergence of Arctic amplification *Geophys. Res. Lett.* **48** e2021GL094086
- England M R, Polvani L M, Screen J and Chan A C 2025 Minimal Arctic sea ice loss in the last 20 years, consistent with internal climate variability *Geophys. Res. Lett.* **52** e2025GL116175
- England M, Jahn A and Polvani L 2019 Nonuniform contribution of internal variability to recent Arctic sea ice loss *J. Clim.* **32** 4039–53
- European Centre for Medium-Range Weather Forecasts 2019, updated monthly ERA5 Reanalysis (0.25 Degree Latitude-Longitude Grid) (Research Data Archive at the National Center for Atmospheric Research, Computational and Information Systems Laboratory) (<https://doi.org/10.5065/BH6N-5N20>) (Accessed 12 May 2024)
- Francis J A and Hunter E 2007 Drivers of declining sea ice in the Arctic winter: a tale of two seas *Geophys. Res. Lett.* **34** L17503
- Garcia-Olivé L, Counillon F, Bethke I and Keenlyside N 2024 Intercomparison of initialization methods for seasonal-to-decadal climate predictions with the NorCPM *Clim. Dyn.* **62** 5425–44
- Gilbert A 2025a Gilbertcloud/arctic-wind-contribution: Published version of code and namelists after 1st round of revisions *Zenodo [code]* (<https://doi.org/10.5281/zenodo.16884086>)
- Gilbert A 2025b Observed winds alone cannot explain recent Arctic warming and sea ice loss *Zenodo [dataset]* (<https://doi.org/10.5281/zenodo.16878063>)
- Gillett N P, Stone D A, Stott P A, Nozawa T, Karpechko A Y, Hegerl G C, Wehner M F and Jones P D 2008 Attribution of polar warming to human influence *Nat. Geosci.* **1** 750–4
- GISTEMP Team 2024 GISS Surface Temperature Analysis (GISTEMP), version 4 (NASA Goddard Institute for Space Studies) (available at: <https://data.giss.nasa.gov/gistemp/>)
- Graham R M, Hudson S R and Maturilli M 2019 Improved performance of ERA5 in Arctic gateway relative to four global atmospheric reanalyses *Geophys. Res. Lett.* **46** 6138–47
- Greatbatch R J, Gollan G, Jung T and Kunz T 2012 Factors influencing Northern Hemisphere winter mean atmospheric circulation anomalies during the period 1960/61 to 2001/02 *Quart. J. R. Meteor. Soc.* **138** 1970–82
- Griffies S M et al 2014 An assessment of global and regional sea level for years 1993–2007 in a suite of interannual CORE-II simulations *Ocean Modelling* **78** 35–89
- Griffies S M et al 2016 OMIP contribution to CMIP6: experimental and diagnostic protocol for the physical component of the Ocean Model Intercomparison project *Geosci. Model Dev.* **9** 3231–96
- He S, Xu X, Furevik T and Gao Y 2020 Eurasian cooling linked to the vertical distribution of Arctic warming *Geophys. Res. Lett.* **47** e2020GL087212
- Hersbach H et al 2020 The ERA5 global reanalysis *Quart. J. R. Meteor. Soc.* **146** 1999–2049
- Holland M M and Bitz C M 2003 Polar amplification of climate change in coupled models *Clim. Dyn.* **21** 221–32
- Holland M M and Landrum L 2021 The emergence and transient nature of Arctic amplification in coupled climate models *Front. Earth Sci.* **9** 719024
- Holland M M and Stroeve J 2011 Changing seasonal sea ice predictor relationships in a changing Arctic climate *Geophys. Res. Lett.* **38** L18501
- Jahn A, Holland M M and Kay J E 2024 Projections of an ice-free Arctic Ocean *Nat. Rev. Earth Environ.* **5** 164–76
- Kay J E et al 2022 Less surface sea ice melt in the CESM2 improves Arctic sea ice simulation with minimal non-polar climate impacts *J. Adv. Model. Earth Syst.* **14** e2021MS002679

- Kay J E, Holland M M and Jahn A 2011 Inter-annual to multi-decadal Arctic sea ice extent trends in a warming world *Geophys. Res. Lett.* **38** L15708
- Kirchmeier-Young M C, Zwiers F W and Gillett N P 2017 Attribution of extreme events in Arctic sea ice extent *J. Clim.* **30** 553–71
- Labe Z, Peings Y and Magnusdottir G 2020 Warm Arctic, cold Siberia pattern: role of full Arctic amplification versus sea ice loss alone *Geophys. Res. Lett.* **47** e2020GL088583
- Lenssen N, Schmidt G A, Hendrickson M, Jacobs P, Menne M J and Ruedy R 2024 A NASA GISTEMPv4 observational uncertainty ensemble *J. Geophys. Res. Atmos.* **129** e2023JD040179
- Luo B, Luo D, Wu L, Zhong L and Simmonds I 2017 Atmospheric circulation patterns which promote winter Arctic sea ice decline *Environ. Res. Lett.* **12** 054017
- Luo D, Xiao Y, Yao Y, Dai A, Simmonds I and Franzke C L E 2016 Impact of ural blocking on winter warm Arctic-Cold Eurasian Anomalies. Part I: blocking-induced amplification *J. Clim.* **29** 3925–47
- Manabe S and Stouffer R J 1980 Sensitivity of a global climate model to an increase of CO₂ concentration in the atmosphere *J. Geophys. Res. Oceans* **85** 5529–54
- Massonnet F, Vancoppenolle M, Goosse H, Docquier D, Fichefet T and Blanchard-Wrigglesworth E 2018 Arctic sea-ice change tied to its mean state through thermodynamic processes *Nat. Clim. Change* **8** 599–603
- McIlholland E A and L'Ecuyer T S 2025 Improved Arctic near-surface air temperatures in CESM2 relative to surface station and buoy measurements *J. Clim.* **38** 4589–610
- Meier W, Fetterer F, Windnagel A and Stewart S 2021 NOAA/NSIDC climate data record of passive microwave sea ice concentration, version 4 (<https://nsidc.org/data/g02202/versions/4/>)
- Min S K, Zhang X, Zwiers F W and Agnew T 2008 Disentangling leaf area and environmental effects on the response of the net ecosystem CO₂ exchange to diffuse radiation *Geophys. Res. Lett.* **35** L16805
- Mueller B L, Gillett N P, Monahan A H and Zwiers F W 2018 Attribution of Arctic sea ice decline from 1953 to 2012 to influences from natural, greenhouse gas and anthropogenic aerosol forcing *J. Clim.* **31** 7771–87
- Najafi M R, Zwiers F W and Gillett N P 2015 Attribution of Arctic temperature change to greenhouse-gas and aerosol influences *Nat. Clim. Change* **5** 246–9
- Ogi M and Wallace J M 2007 Summer minimum Arctic sea ice extent and the associated summer atmospheric circulation *Geophys. Res. Lett.* **34** L12705
- Overland J, Francis J A, Hall R, Hanna E, Kim S J and Vihma T 2015 The melting Arctic and midlatitude weather patterns: are they connected? *J. Clim.* **28** 7917–32
- Pernov J B, Gros-Daillon J and Schmale J 2024 Comparison of selected surface level ERA5 variables against in-situ observations in the continental Arctic *Quart. J. R. Meteor. Soc.* **150** 2123–46
- Räisänen J 2021 Effect of atmospheric circulation on surface air temperature trends in years 1979–2018 *Clim. Dyn.* **56** 2303–20
- Rantanen M, Karpeckha A Y, Lippinen A, Nordling K, Hyvärinen O, Ruosteenoja K, Vihma T and Laaksonen A 2022 The Arctic has warmed nearly four times faster than the globe since 1979 *Commun. Earth Environ.* **3** 1–10
- Roach L A and Blanchard-Wrigglesworth E 2022 Observed winds crucial for September Arctic sea ice loss *Geophys. Res. Lett.* **49** e2022GL097884
- Roach L A, Blanchard-Wrigglesworth E, Ragen S, Cheng W, Armour K C and Bitz C M 2022 The impact of winds on AMOC in a fully-coupled climate model *Geophys. Res. Lett.* **49** e2022GL101203
- Screen J A and Simmonds I 2010 The central role of diminishing sea ice in recent Arctic temperature amplification *Nature* **464** 1334–7
- Serreze M C, Barrett A P, Stroeve J C, Kindig D N and Holland M M 2009 The emergence of surface-based Arctic amplification *Cryosphere* **3** 11–19
- Siew P Y F, Wu Y, Ting M, Zheng C, Ding Q and Seager R 2024 Significant contribution of internal variability to recent Barents–Kara sea ice loss in winter *Commun. Earth Environ.* **5** 411
- Simmonds I 2015 Comparing and contrasting the behaviour of Arctic and Antarctic sea ice over the 35 year period 1979–2013 *Ann. Glaciol.* **56** 18–28
- Stroeve J C, Kattsov V, Barrett A, Serreze M, Pavlova T, Holland M and Meier W N 2012 Trends in Arctic sea ice extent from CMIP5, CMIP3 and observations *Geophys. Res. Lett.* **39** L16502
- Sweeney A J, Fu Q, Po-Chedley S, Wang H and Wang M 2023 Internal variability increased Arctic amplification during 1980–2022 *Geophys. Res. Lett.* **50** e2023GL106060
- Topál D and Ding Q 2023 Atmospheric circulation-constrained model sensitivity recalibrates Arctic climate projections *Nat. Clim. Change* **13** 710–8
- Tsujino H et al 2020 Evaluation of global ocean–sea-ice model simulations based on the experimental protocols of the Ocean Model Intercomparison Project phase 2 (OMIP-2) *Geosci. Model Dev.* **13** 3643–708
- Webster M A, Du Vivier A K, Holland M M and Bailey D A 2021 Snow on Arctic sea ice in a warming climate as simulated in CESM J. *Geophys. Res. Oceans* **126** e2020JC016308
- Wettstein J J and Deser C 2014 Internal variability in projections of twenty-first-century Arctic sea ice loss: role of the large-scale atmospheric circulation *J. Clim.* **27** 527–50
- Wilks D S 2016 The stippling shows statistically significant grid points”: how research results are routinely overstated and overinterpreted and what to do about it *Bull. Am. Meteor. Soc.* **97** 2263–73
- Xu X, He S, Gao Y, Furevik T, Wang H, Li F and Ogawa F 2019 Strengthened linkage between midlatitudes and Arctic in boreal winter *Clim. Dyn.* **53** 3971–83
- Zhang J, Lindsay R, Schweiger A and Steele M 2013 The impact of an intense summer cyclone on 2012 Arctic sea ice retreat *Geophys. Res. Lett.* **40** 720–6